

## Vav2 Is an Activator of Cdc42, Rac1, and RhoA\*

(Received for publication, August 19, 1999, and in revised form, January 10, 2000)

Karon Abe<sup>‡§</sup>, Kent L. Rossman<sup>¶</sup>, Betty Liu<sup>||</sup>, Kimberly D. Ritola<sup>‡</sup>, Derek Chiang<sup>¶</sup>,  
Sharon L. Campbell<sup>¶</sup>, Keith Burridge<sup>||</sup>, and Channing J. Der<sup>‡\*\*</sup>

From the Departments of <sup>‡</sup>Pharmacology, <sup>¶</sup>Biochemistry and Biophysics, and <sup>||</sup>Cell Biology and Anatomy, Lineberger Comprehensive Cancer Center, University of North Carolina, Chapel Hill, North Carolina 27599

**Vav and Vav2 are members of the Dbl family of proteins that act as guanine nucleotide exchange factors (GEFs) for Rho family proteins. Whereas Vav expression is restricted to cells of hematopoietic origin, Vav2 is widely expressed. Although Vav and Vav2 share highly related structural similarities and high sequence identity in their Dbl homology domains, it has been reported that they are active GEFs with distinct substrate specificities toward Rho family members. Whereas Vav displayed GEF activity for Rac1, Cdc42, RhoA, and RhoG, Vav2 was reported to exhibit GEF activity for RhoA, RhoB, and RhoG but not for Rac1 or Cdc42. Consistent with their distinct substrate targets, it was found that constitutively activated versions of Vav and Vav2 caused distinct transformed phenotypes when expressed in NIH 3T3 cells. In contrast to the previous findings, we found that Vav2 can act as a potent GEF for Cdc42, Rac1, and RhoA *in vitro*. Furthermore, we found that NH<sub>2</sub>-terminally truncated and activated Vav and Vav2 caused indistinguishable transforming actions in NIH 3T3 cells that required Cdc42, Rac1, and RhoA function. In addition, like Vav and Rac1, we found that Vav2 activated the Jun NH<sub>2</sub>-terminal kinase cascade and also caused the formation of lamellipodia and membrane ruffles in NIH 3T3 cells. Finally, Vav2-transformed NIH 3T3 cells showed up-regulated levels of Rac-GTP. We conclude that Vav2 and Vav share overlapping downstream targets and are activators of multiple Rho family proteins. Therefore, Vav2 may mediate the same cellular consequences in nonhematopoietic cells as Vav does in hematopoietic cells.**

active GTP-bound protein, Rho family proteins are inactivated by GTPase-activating proteins (GAPs) that stimulate the intrinsic rate of GTP hydrolysis. A wide array of extracellular stimuli has been shown to promote the activation of Rho family proteins, most likely through the activation of Dbl family proteins.

Fourteen mammalian members of the Rho family of proteins have been identified: RhoA, RhoB, RhoC, RhoD, RhoE, Rnd1/Rnd6, Rnd2/Rho7, RhoG, Rac1, Rac2, Rac3, Cdc42, TC10, and TTF (5). Rho family proteins have been shown to regulate actin cytoskeletal organization, thus influencing cell shape, adhesion, and motility (reviewed in Refs. 3–5). For example, RhoA promotes the formation of actin stress fibers and focal adhesions, whereas Rac1 promotes the formation of lamellipodia and membrane ruffling, and Cdc42 causes actin microspike formation and filopodia development.

Rho family proteins are also activators of signaling pathways that regulate gene expression and cell growth (3–5). For example, Rac1 and Cdc42 but not RhoA activate the Jun NH<sub>2</sub>-terminal kinase (JNK) mitogen-activated protein kinase cascade, and JNK in turn phosphorylates and activates the Jun, ATF-2 and Elk-1 transcription factors (6, 7). RhoA, Rac1, and Cdc42 are also activators of the NF- $\kappa$ B and serum response factor transcription factors (8, 9). These transcription factors in turn regulate genes that promote cell growth. Rho family proteins are also required for progression through the G<sub>1</sub> phase of the cell cycle, in part, by up-regulating the expression of cyclin D1 (10, 11). Thus, it is not surprising that the aberrant activation of Rho family proteins can promote cellular transformation, and the proteins are required for the transforming actions of Ras and other oncoproteins.

To date, over 30 mammalian Dbl family members have been identified. All Dbl family proteins share a tandem Dbl homology (DH) and pleckstrin homology (PH) domain structure (reviewed in Refs. 1 and 2). The DH domain serves as the GTPase binding and GEF catalytic domain. Whereas some Dbl proteins show very specific substrate specificity, others show broad substrate specificity. For example, the Dbl family proteins Lsc, Fdg1, and Tiam1 are specific for RhoA, Cdc42, and Rac1, respectively (12–14). In contrast, Vav has been found to activate multiple Rho family proteins (Rac1, RhoA, RhoB, RhoG, and Cdc42) (15–18). Although the structural basis for substrate specificity of DH domains remains to be delineated, we have observed that the overall sequence identities of DH domains does broadly correlate with their GTPase targets (2).

Although PH domains are found in other signaling proteins, a PH domain is invariantly positioned just COOH-terminal to the DH domain within Dbl family proteins (1, 2). Thus, the tandem DH/PH association suggests that these domains may be functionally interdependent. Presently, it is believed that the PH domain facilitates the membrane localization of Dbl family proteins, where their GTPase substrates reside (19, 20). A second function involves the positive or negative regulation

Dbl family proteins serve as guanine nucleotide exchange factors (GEFs)<sup>1</sup> and activators of specific Rho family small GTPases (reviewed in Refs. 1 and 2). Rho family proteins function as GDP/GTP-regulated molecular switches that cycle between an active GTP-bound state and an inactive GDP-bound state (reviewed in Refs. 3–5). Whereas Dbl family proteins stimulate GDP dissociation to promote the formation of the

\* This work was supported by National Institutes of Health Grants CA42978, CA55008, and CA63071 (to C. J. D.) and GM29860 (to K. B.). The costs of publication of this article were defrayed in part by the payment of page charges. This article must therefore be hereby marked "advertisement" in accordance with 18 U.S.C. Section 1734 solely to indicate this fact.

§ Recipient of a Butler Fellowship Award.

\*\* To whom correspondence should be addressed: University of North Carolina at Chapel Hill, Lineberger Comprehensive Cancer Center, CB# 7295, Chapel Hill, NC 27599-7295. Tel.: 919-966-5634; Fax: 919-966-0162; E-mail: [cjder@med.unc.edu](mailto:cjder@med.unc.edu).

<sup>1</sup> The abbreviations used are: GEF, guanine nucleotide exchange factor; DH, Dbl homology; PH, pleckstrin homology; CRD, cysteine-rich domain; JNK, c-Jun NH<sub>2</sub>-terminal kinase; SH2, Src homology 2; SH3, Src homology 3; GAP, GTPase-activating protein; GBD, GTP-binding domain; GST, glutathione S-transferase; mant, N-methylanthranilyl.

of the catalytic function of the DH domain (21–23). Outside the DH domains, Dbl family members generally share little sequence similarity. Because NH<sub>2</sub>-terminal deletion of sequences upstream of the DH domain creates transforming versions of various Dbl family proteins (e.g. Vav, Dbl, and Tiam1), the NH<sub>2</sub>-terminal sequences may serve a negative regulatory role for these proteins.

A majority of Dbl family proteins have been shown to exhibit transforming potential in NIH 3T3 focus formation assays: Dbl, Vav, Dbs, Ost, Ect2, Net1, Tim, Lbc, Lsc, Lfc, Tiam1, Trio, and Fgd1 (1, 2). Several lines of evidence indicate that Dbl family transformation is the result of their deregulation of Rho GTPase activity. First, where it has been analyzed, mutation of the DH domain causes a loss of transforming activity. Second, Dbl family proteins cause the same changes in actin cytoskeletal organization as their small GTPase substrates. Third, constitutively activated Rho GTPases and Dbl family proteins cause very similar transformed phenotypes when assayed in rodent fibroblasts and other cell types. Fourth, Dbl family members can activate similar signaling pathways as their Rho GTPase substrates. Thus, the activation of Rho GTPases plays an important role in Dbl transformation.

Vav and Vav2 are members of the Dbl family of proteins. These two proteins are highly related showing 63% sequence similarity and 55% identity (24, 25). In particular, among all Dbl family proteins, the DH domain of Vav2 shares the strongest sequence identity with that of Vav. The transforming activity of both Vav and Vav2 can be activated by NH<sub>2</sub>-terminal truncation (25, 26). Both proteins also contain the same spectrum of COOH-terminal protein-protein or protein-lipid interaction motifs. Following the PH domain is a cysteine-rich domain and tandem Src homology 3 (SH3) domains split by an intervening SH2 domain. However, Vav and Vav2 are also distinct in several ways. First, whereas Vav expression is restricted to hematopoietic cells, Vav2 is expressed ubiquitously. Second, although Vav has shown GEF activity on RhoA, RhoG, Rac1, and Cdc42 *in vitro* (15, 16, 18), Vav2 has recently been reported to have GEF activity on RhoA, RhoB, and RhoG but not on Rac1 and Cdc42 *in vitro* (18). Furthermore, Vav and Vav2 were also demonstrated to have distinct consequences on cell morphology and actin organization and caused distinct transformed phenotypes that correlated with their different substrate specificity. Thus, it has been proposed that Vav and Vav2 may be activated by similar upstream stimuli but then stimulate distinct downstream signaling events and biological outcomes.

We have evaluated the biochemical and biological properties of Vav2. In contrast to previous observations, we found that Vav2 is an activator of RhoA, Rac1, and Cdc42. Similar to Vav, Vav2 (a DH or DH/PH/CRD fragment) exhibited potent guanine nucleotide exchange activity on RhoA, Rac1, and Cdc42 *in vitro*. Consistent with this exchange activity, Vav2 caused a similar transformed phenotype as Vav when expressed in NIH 3T3 cells. Furthermore, like Vav, Vav2 transforming activity was impaired by inhibition of RhoA, Rac1, and Cdc42 function. Like Rac1, Vav2 also induced the formation of lamellipodia and membrane ruffles in NIH 3T3 cells. Vav2 also stimulated the activity of the c-Jun transcription factor, a signaling pathway activated by Rac or Cdc42. Finally, Vav2-transformed NIH 3T3 cells showed a significant increase in the levels of Rac-GTP. Thus, when taken together, our data suggest that Vav2 can activate multiple Rho GTPases similar to its related family member Vav.

#### EXPERIMENTAL PROCEDURES

**Molecular Constructs**—The pAX142 mammalian expression plasmid (20) and pAX142  $\Delta$ N-186 *vav* have been described previously (27). The

$\Delta$ N-191 Vav2 mutant was generated by polymerase chain reaction using wild-type full-length Vav2 (pCMV5-*vav2*; a generous gift from Dan Broek) as a template. A 5' primer (CA GGT ACC GGC ATG ACT GAA GAT GAC AAG) containing a *Kpn*I site and seven Vav2 NH<sub>2</sub>-terminal residues corresponding to residues 192–198 was used in conjunction with a 3' primer (CA GGT ACC GGC GTC CAG ATC TGC AGG AGA) containing a *Kpn*I and a *Bgl*II site (the *Bgl*II site corresponds to residue 578 in Vav2) to generate a 1.7-kilobase fragment. This fragment was digested with *Kpn*I and ligated into a *Kpn*I-digested pCMV5-*vav2* plasmid. This plasmid containing the polymerase chain reaction-generated fragment was then sequenced. The pCMV5-*vav2* + insert fragment was digested with *Bgl*II, and the larger vector fragment was recovered and religated together (pCMV5  $\Delta$ N-191*vav2*). To compare  $\Delta$ N-186 Vav and  $\Delta$ N-191 Vav2 transforming activities, pCMV5  $\Delta$ -191*vav2* was digested with *Kpn*I and *Hind*III, converted to blunt ends using T4 DNA polymerase (Life Technologies, Inc.), and ligated into the *Sma*I site in pAX142.

pZIP-NeoSV(x)1 retrovirus mammalian expression constructs encoding wild-type or dominant negative mutants of RhoA, Rac1, or Cdc42, and Rho GAP p190 have been described and characterized previously (28). cDNAs encoding wild-type p190 Rho GAP (29) and C3 transferase were provided by R. Weinberg and J. Settleman, respectively. pyDF30 WASP-GBD encodes the NH<sub>2</sub>-terminal sequences of WASP that contains the Cdc42-GBD and WASP-GBD has been shown to function as an inhibitor of Cdc42 function (provided by M. Symons) (10, 30, 31).

**Cell Culture, Transfection, and Transformation Assays**—NIH 3T3 cells were maintained in Dulbecco's modified Eagle medium supplemented with 10% bovine calf serum. Transfections were performed using calcium phosphate co-precipitation in conjunction with glycerol shock as described previously (32). For each assay, cognate empty vector was used as a control. For focus formation analyses, transfected NIH 3T3 cells were maintained in growth medium for 12–14 days. The cultures were then stained with crystal violet (0.5%), and the number of foci of transformed cells was then quantitated. To select for NIH 3T3 cells stably expressing constitutively activated Vav2, pAX142  $\Delta$ N191-Vav2 (1  $\mu$ g) were co-transfected with the pZIP-NeoSV(x)1 empty plasmid (neomycin resistant) and maintained in growth medium supplemented with G418 (400  $\mu$ g/ $\mu$ l). NIH 3T3 cells stably expressing constitutively activated Vav by transfection of pCTV3  $\Delta$ N-186 Vav and selection of stably transfected cells were established by isolating drug-resistant colonies after growth in medium supplemented with hygromycin. Multiple drug resistant colonies (>100) were pooled together to establish the stable cell lines for use in the various assays described. Anchorage-independent growth assays were performed as described previously (32). For immunofluorescence analyses, NIH 3T3 fibroblasts were transfected with 2  $\mu$ g of cognate mammalian expression vector pAX142, pAX142  $\Delta$ N-186 Vav, or pAX142  $\Delta$ N-191 Vav2 using the LipofectAMINE Plus (Life Technologies, Inc.) reagent according to manufacturer's instructions. 24 h after transfection, cells were trypsinized and plated on 10  $\mu$ g/ml fibronectin-coated glass coverslips (Carolina Biologicals) and allowed to attach and spread for 2 h.

**Transient Expression Reporter Gene Assays**—NIH 3T3 cells were transfected by calcium phosphate co-precipitation as described previously (32). 48 h after transfection, cells were starved for 15 h with Dulbecco's modified Eagle medium supplemented with 0.5% bovine calf serum to reduce the level of serum activation of c-Jun. Analyses of the cell lysates of the transiently transfected NIH 3T3 cells were performed using enhanced chemiluminescence reagents and a Monolight 2010 luminometer (Analytical Luminescence) as described previously (33, 34). The reporter constructs utilized were previously described; Gal4-Jun encodes the Gal4 DNA-binding domain fused to the NH<sub>2</sub>-terminal transactivation domain of c-Jun (35), and 5xGal4-Luc contains the luciferase gene under control of tandem copies of the Gal4 DNA-binding sequences and the minimal promoter of *c-fos*.

**Guanine Nucleotide Exchange Assays**—cDNA fragments encoding either the human Vav2 DH domain (residues 191–402) or the tandem DH/PH/CRD (residues 191–573) were generated by polymerase chain reaction and inserted into the *Nco*I/*Xho*I sites of the bacterial expression vector pET-28a (Novagen). The bacterial expression constructs were transformed into the *Escherichia coli* strain BL21 (DE3), and protein expression was induced with 1 mM IPTG at 25 °C. The recombinant proteins were His<sub>6</sub>-tagged at its COOH terminus and were purified from bacterial lysate on a nickel-nitrilotriacetic acid agarose column (Qiagen). The Vav2 DH protein was further purified on a S-200 size exclusion column (Amersham Pharmacia Biotech) and a source-Q anion exchange column (Amersham Pharmacia Biotech). A similar bacterial expression vector encoding the isolated DH domain of Dbs has been previously described (20). Bacterially expressed Tiam1 DH/PH

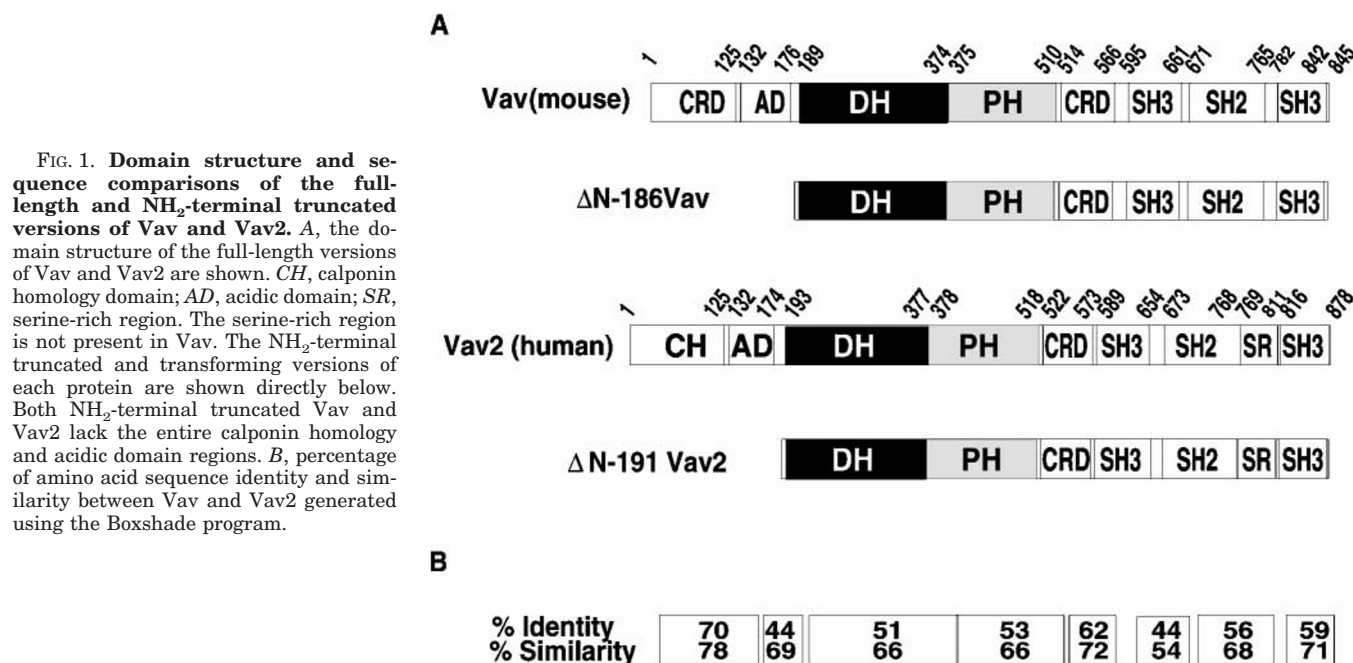


**FIG. 1. Domain structure and sequence comparisons of the full-length and NH<sub>2</sub>-terminal truncated versions of Vav and Vav2.** *A*, the domain structure of the full-length versions of Vav and Vav2 are shown. *CH*, calponin homology domain; *AD*, acidic domain; *SR*, serine-rich region. The serine-rich region is not present in Vav. The NH<sub>2</sub>-terminal truncated and transforming versions of each protein are shown directly below. Both NH<sub>2</sub>-terminal truncated Vav and Vav2 lack the entire calponin homology and acidic domain regions. *B*, percentage of amino acid sequence identity and similarity between Vav and Vav2 generated using the Boxshade program.

protein was kindly provided by J. Sondek. Bacterially expressed GST-RhoA(F25N), GST-Rac1(WT), and GST-Cdc42(WT) were expressed and purified essentially as described (36). Bacterially expressed Ha-Ras (1–166) was purified as described previously (37).

The GDP dissociation assays were carried out by the filter binding method that was described previously (38). To prepare [<sup>3</sup>H]GDP-loaded GST-Rho, GST-Rac, or GST-Cdc42, solutions containing 10 mM HEPES, pH 7.5, 100 mM NaCl, 7.5 mM EDTA, 15 μM GDP, 5.5 μM [<sup>3</sup>H]GDP, and 12.5 μM of the GTPase were incubated for 25 min at 20 °C. The [<sup>3</sup>H]GDP-bound GTPases were then stabilized by supplementing the solution with 20 mM MgCl<sub>2</sub>. Nucleotide exchange reactions were performed at 20 °C by diluting the [<sup>3</sup>H]GDP-loaded GST-RhoA, GST-Rac1, or GST-Cdc42 to 4 μM in reaction mixtures containing either 4 μM GEF (Vav2 DH, Dbs DH, Tiam1 DH/PH) or no GEF, 10 mM HEPES, pH 7.5, 5 mM MgCl<sub>2</sub>, 100 mM NaCl, 1 mM dithiothreitol, 50 μg/ml bovine serum albumin, and 100 μM GTP (final concentrations). 30 μl of each reaction mixture were sampled at 0, 5, 10, and 20 min and quenched in 1 ml of ice-cold dilution buffer containing 20 mM Tris, pH 7.5, 100 mM NaCl, and 20 mM MgCl<sub>2</sub>. The amount of [<sup>3</sup>H]GDP remaining bound to the GTPases was measured by filtering the quenched samples over nitrocellulose followed by scintillation counting. The percentage of [<sup>3</sup>H]GDP remaining bound at each time point for the GEF catalyzed and uncatalyzed reactions were evaluated relative to time 0 of the uncatalyzed reaction. Dbs DH and Tiam1 DH/PH were included as positive controls for GST-Cdc42 and GST-Rac1, respectively. Results are the average of two independent assays.

Fluorescence spectroscopic analysis of *N*-methylanthraniloyl (mant)-GDP incorporation into GDP-preloaded GST-Rac1, GST-Cdc42, GST-RhoA, or Ha-Ras was carried out using a Perkin-Elmer LS 50 B Spectrometer at 20 °C similar to as described previously (39). Exchange reaction assay mixtures containing 20 mM Tris, pH 7.5, 50 mM NaCl, 10 mM MgCl<sub>2</sub>, 1 mM dithiothreitol, 50 μg/μl bovine serum albumin, 1% glycerol, 400 nM mant-GDP (Biomol), and 2 μM of GTPase were prepared and allowed to equilibrate with continuous stirring. After equilibration, the Vav2 DH/PH/CRD polypeptide was added to 50 nM, and the relative mant fluorescence ( $\lambda_{\text{ex}} = 360 \text{ nm}$ ,  $\lambda_{\text{em}} = 440 \text{ nm}$ ) was monitored. Experiments were performed in duplicate.

**Immunofluorescence Analyses**—NIH 3T3 fibroblasts were essentially processed for immunofluorescence as described previously (40). Briefly, cells were fixed in 3.7% formaldehyde in phosphate-buffered saline for 10 min, rinsed in Tris-buffered saline at pH 7.6 for 3 min, and permeabilized for 6 min in Tris-buffered saline containing 0.5% Triton X-100. Expression of the DNA constructs was determined by staining with mouse anti-Vav1 antibody (Upstate Technology, Lake Placid, NY) or rabbit anti-Vav2 antibody generated against the COOH-terminal of Vav2<sup>2</sup> followed by secondary antibodies conjugated to fluorescein iso-

thiocyanate or Texas Red (Chemicon). Actin was visualized with Texas Red-labeled phalloidin (Molecular Probes). Images were acquired through a Micromax 5 MHz cooled CCD camera (Princeton Instrument) on an Axiophot (Zeiss) microscope.

## RESULTS

**Vav2 Demonstrates GEF Exchange Activity on RhoA, Rac1, and Cdc42 in Vitro**—The Vav and Vav2 DH domains share strong sequence identity (51%) (24, 25) (Fig. 1). Furthermore, our sequence alignment and dendrogram analyses of DH domains showed that related DH domains shared similar substrate specificity (2). Therefore, the recent report that Vav2 showed distinct GEF activities from Vav was unexpected (18).

To further evaluate the activity of the DH domain of Vav2, we constructed, expressed, and purified a bacterially expressed hexahistidine-tagged DH domain fragment of Vav2 (residues 191–401) and analyzed the effect of this protein on the incorporation of cold GTP into [<sup>3</sup>H]GDP-loaded RhoA, Rac1, or Cdc42 (Fig. 2). RhoA, Rac1, or Cdc42 alone did not exhibit significant intrinsic GDP dissociation. However, the Vav2 DH domain stimulated rapid and complete GDP dissociation from RhoA, Rac1, and Cdc42 within ~20 min. In fact, the reaction went to completion in 5 min with both Rac1 and Cdc42, whereas only 25% of the [<sup>3</sup>H]GDP was released from RhoA after the same time period. These assays were performed at both stoichiometric and substoichiometric conditions (data not shown). Furthermore, as controls, we examined the *in vitro* GEF exchange activities of Dbl family members Dbs (DH domain) and Tiam-1 (DH/PH domain) on their respective GTPases, Cdc42 and Rac1 (14, 20). We found that Vav2 had similar exchange activities on Rac1 and Cdc42, as did Tiam-1 and Dbs, respectively. Finally, unlike proto-Vav and onco-Vav (deletion of residues 1–67), which require phosphorylation for efficient GEF activity *in vitro* (15, 16), the catalytic activity of the isolated DH domain of Vav2 was not only more efficient than previously observed for Vav but was also phosphorylation-independent. Therefore, in our assays, we found that Vav2, like Vav, displayed *in vitro* substrate specificities toward RhoA, Rac1, and Cdc42. Moreover, we found that Vav2 displayed comparable activity for Rac1 and Cdc42 and lower activity for RhoA.

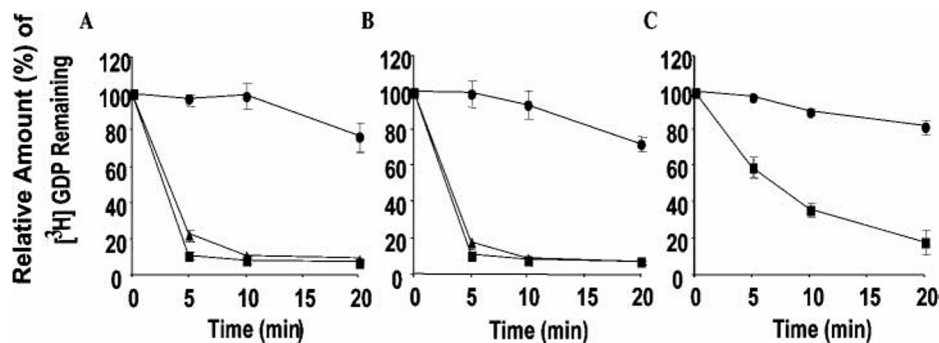


FIG. 2. **Stimulation of GDP dissociation from Cdc42, Rac1, and RhoA from Vav2.** Time course study for the dissociation of [ $^3\text{H}$ ]GDP from the bacterially expressed GST-Rac1 (A), GST-Cdc42 (B), or GST-RhoA (C) in the presence of a bacterial expressed Vav2 DH domain fragment. A, Tiam1 has been shown to specifically catalyze GTPase exchange activity on Rac1; hence, we used a bacterially expressed DH/PH domain fragment of Tiam1 as a control to compare with Vav2 utilization of Rac1. We also used a bacterially expressed DH domain fragment of DbS as a control (B) that catalyzes GDP dissociation on Cdc42 (and RhoA). Experiments shown are representative of two independent assays that were performed in duplicate. Symbols: A, ●, Rac1; ■, Vav2 + Rac1; ▲, Tiam1 + Rac1; △, DbS + Cdc42; B, ●, Cdc42; ■, Vav2 + Cdc42; ▲, DbS + Cdc42; C, RhoA; ■, Vav2 + RhoA.

Because sequences flanking the DH domain may influence DH domain substrate specificity, we also evaluated the activity of a bacterially expressed fragment of Vav2 that contains the DH domain together with the COOH-terminal PH and cysteine-rich domains (designated DH/PH/CRD). We have found that the equivalent version of Vav (DH/PH/CRD) is functional *in vivo* for signaling and transforming activity (48). For these analyses we employed a fluorescence spectroscopic analysis of mant-GDP incorporation into GDP-preloaded Rac1, Cdc42, RhoA, and Ha-Ras bacterially expressed proteins (Fig. 3). Similar to our observations with the DH domain alone, we found that the DH/PH/CRD polypeptide displayed comparable activity for Rac1 and Cdc42, lower activity for RhoA, and no activity for Ha-Ras. Thus, the addition of flanking COOH-terminal sequences required for Vav DH domain activity *in vivo* did not alter the GTPase specificity of the Vav2 DH domain.

**Vav and Vav2 Cause Indistinguishable Transformed Phenotypes in NIH 3T3 Cells**—In contrast to previous analyses (18), our *in vitro* analyses showed that Vav2 does act as a GEF for Rac1 and Cdc42, as well as RhoA, *in vitro*. The previous study also found that Vav and Vav2 caused distinct transformed phenotypes when expressed in NIH 3T3 cells (18, 25). For example, whereas Vav caused the appearance of foci of transformed cells that consisted of piled up, nonrefractile cells, Vav2 was reported to cause the appearance of foci that contained multinucleated cells that included rounded and refractile cells. This was consistent with their observed differences in Vav and Vav2 substrate specificity. However, because our analyses showed that Vav and Vav2 displayed the same substrate specificity, we next determined whether Vav and Vav2 caused similar or distinct transformation phenotypes.

For these analyses, we used an NH<sub>2</sub>-terminal truncated mutant of mouse Vav,  $\Delta\text{N-186 Vav}$ , which lacks NH<sub>2</sub>-terminal residues 1–186 (Fig. 1). We recently showed that this mutant of Vav is several 100-fold more potent in focus-forming activity when compared with the originally cloned onco-Vav (deletion of residues 1–67) (27). We also generated an equivalent version of human Vav2 by deleting residues 1–191 from its NH<sub>2</sub> terminus (designated  $\Delta\text{N-191 Vav2}$ ) (Fig. 1). Thus, both these mutants lack the entire NH<sub>2</sub>-terminal sequences upstream of the DH domain. A similar truncation mutant of Vav2 lacking residues 1–184 was shown previously to transform NIH 3T3 cells (25).

Like  $\Delta\text{N-186 Vav}$ ,  $\Delta\text{N-191 Vav2}$  showed potent focus-forming activity when transfected into NIH 3T3 cells ( $\sim 40$  foci/ $\mu\text{g}$  of DNA). The transformed foci caused by  $\Delta\text{N-191 Vav2}$  were indistinguishable in appearance from those caused by  $\Delta\text{N-186 Vav}$  and consisted of dense clusters of nonrefractile cells (Fig. 4A). These foci were similar to those caused by activated forms

of RhoA or Rac1 but very distinct from those caused by activated Ras or by activated serine/threonine or tyrosine kinases (not shown). We observed no multi-nucleated giant cells for either the Vav- or Vav2-induced foci.

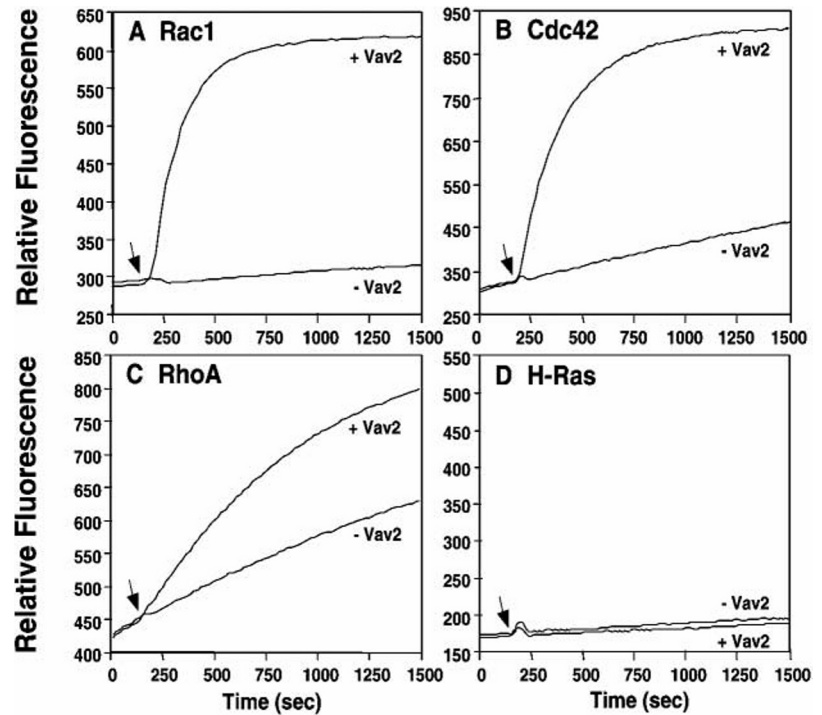
We then compared the morphology of NIH 3T3 cells stably expressing activated Vav or Vav2. Both caused equivalent consequences on cellular morphology (Fig. 4B).  $\Delta\text{N-186 Vav}$ - and  $\Delta\text{N-191 Vav2}$ -transformed cells exhibited a nonrefractile, strongly adherent appearance that was slightly more elongated than the vector-transfected, untransformed NIH 3T3 cells. We also plated NIH 3T3 cells that stably expressed Vav or Vav2 onto soft agar and examined their ability to grow in an anchorage-independent manner (Fig. 4C). We found that similar to cells expressing activated Vav activated Vav2-expressing cells formed colonies in soft agar. Thus, consistent with our data showing similar GEF activities, we observed that activated Vav and Vav2 caused qualitatively and quantitatively similar transformed phenotypes when expressed in NIH 3T3.

**Vav2 Transforming Activity Requires RhoA, Rac1, and Cdc42**—We recently showed that Vav transformation of NIH 3T3 cells required the activity of RhoA, Rac1, and Cdc42 (27). Therefore, to assess the importance of RhoA, Rac1, and Cdc42 function in Vav2 transforming activity, we performed similar experiments using  $\Delta\text{N-191 Vav2}$  using various approaches to inhibit the function of Rho family GTPases.

We co-transfected  $\Delta\text{N-191 Vav2}$  with expression vectors encoding dominant negative mutants RhoA(19N), Rac1(17N), or Cdc42(17N). By analogy to the Ras(17N) dominant negative protein, these dominant negative mutants have been proposed to inhibit Rho family protein function by forming nonproductive interactions with Dbf family members that associate with the Rho GTPase substrate (41–43). We and others have used these mutants to characterize the involvement of specific Rho family GTPases in transformation by various Dbf family proteins (12, 20, 44). Co-expression of dominant negative RhoA(19N), Rac1(17N), or Cdc42(17N) caused significant reductions, ranging from 65 to 90%, in Vav2 focus-forming activity (Fig. 5A).

We also used other approaches to support the inhibition of Vav2 transformation that we observed with the dominant negative Rho GTPase mutants. We co-transfected  $\Delta\text{N-191 Vav2}$  with p190 Rho GAP, a protein that stimulates the intrinsic GTP hydrolysis rate of RhoA (45), as a second approach to evaluate an involvement of RhoA in Vav2 transformation. We also co-transfected  $\Delta\text{N-191 Vav2}$  with a plasmid encoding the C3 botulinum toxin, which specifically inhibits RhoA, RhoB, and RhoC (but not Rac1 or Cdc42) function (Fig. 5B), or with a plasmid encoding the isolated Cdc42 binding domain of WASP,

**FIG. 3. Stimulation of mant-GDP incorporation into Rac1, Cdc42, RhoA, and Ha-Ras by the Vav2 DH/PH/CRD *in vitro*.** The ability of bacterially expressed Vav2 DH/PH/CRD (50 nM) to stimulate the incorporation of mant-GDP into bacterially expressed GTPases (2  $\mu$ M) was measured by fluorescence spectroscopy ( $\lambda_{\text{ex}} = 360$  nm,  $\lambda_{\text{em}} = 440$  nm). **A**, lower curve, GST-Rac1; upper curve, GST-Rac1 + DH/PH/CRD; **B**, lower curve, GST-Cdc42; upper curve, GST-Cdc42 + DH/PH/CRD; **C**, lower curve, GST-RhoA; upper curve, GST-RhoA + DH/PH/CRD; **D**, lower curve, Ha-Ras + DH/PH/CRD; upper curve, Ha-Ras. Arrows indicate the time point at which the Vav2 DH/PH/CRD polypeptide was added to the exchange reaction mixture. Results are representative of two independent assays.



a Cdc42-specific effector (Fig. 5C). This WASP fragment has been utilized as a specific inhibitor of Cdc42 function (10, 30, 31). Co-expression of p190 Rho GAP or C3 decreased Vav2 transforming activity by 90% (Fig. 5, A and B), whereas co-transfection with the WASP fragment decreased Vav2 transforming activity by 50% (Fig. 4C). Taken together with the data from the use of dominant negative GTPases, our observations support a role for RhoA, Rac1, and Cdc42 in mediating Vav2 transforming activity.

**Vav2 Stimulates *c-Jun* Transcriptional Activity**—Vav has been shown to be a strong activator of the JNK mitogen-activated protein kinase and, consequently, the *c-Jun* transcription factor (17, 46). In most cell types, JNK activity is stimulated by activated Rac1 and Cdc42, but not RhoA (6, 7). Therefore, we examined the ability of  $\Delta$ N-191 Vav2 to stimulate *c-Jun* transcriptional activity. For these studies, we performed transient transcriptional assays in NIH 3T3 cells. We transfected cognate empty vector or vectors encoding constitutively activated RhoA(63L), Rac1(61L), or  $\Delta$ N-191 Vav2 and assessed *c-Jun* transcriptional activation (Fig. 6). In our assays, we found that constitutively activated RhoA(63L) did not cause activation of *c-Jun*, whereas both Rac(61L) and Vav2 caused over 3-fold stimulation of *c-Jun* activity.

**Vav2 Induces the Formation of Lamellipodia and Membrane Ruffles**—Previous studies found that Vav and Vav2 caused distinct consequences on actin cytoskeletal organization when stably expressed in NIH 3T3 cells (18). Whereas Vav caused a disruption of stress fibers and a preferential localization of actin to peripheral membrane structures, Vav2 induced the formation of abundant stress fibers. In contrast, their analyses of NIH 3T3 cells transiently expressing Vav or Vav2 showed equivalent consequences, with both causing an induction of lamellipodia and membrane ruffling and no obvious formation of filopodia or stress fibers. However, this activity was distinct from the significantly larger lamellipodia caused by activated Rac1.

For our analyses, we transiently transfected NIH 3T3 cells with  $\Delta$ N-186 Vav,  $\Delta$ N-191 Vav2, or their respective cognate vectors. Cells expressing activated Vav or Vav2 displayed the same consequences on actin organization (Fig. 7) as activated

Rac1 (not shown). When compared with empty vector-transfected NIH 3T3 cells, cells expressing activated Vav or Vav2 were more rounded and displayed lamellipodia and membrane ruffling, indicating that both are activators of Rac1 *in vivo*. In contrast to previous observations (18), we did not see a disruption of actin stress fibers by activated Vav. Instead, both activated Vav- and Vav2-expressing cells retained well developed actin stress fibers that were similar to those seen in untransformed NIH 3T3 cells.

Our observations that Vav2 caused the induction of lamellipodia and membrane ruffling and that dominant negative Rac1 could block Vav2 transforming activity supported the possibility that Vav2 transformation is associated with constitutive up-regulation of Rac1 function. To address this possibility, we utilized a GST fusion protein containing the Cdc42/Rac binding domain of PAK1 (residues 67–150) as an affinity reagent in a pull-down assay to determine the level of GTP-bound Rac in Vav2-transformed NIH 3T3 cells (47–49). The PAK serine/threonine kinase is an effector of both Rac and Cdc42 and binds preferentially to the active, GTP-bound forms of these two GTPases. When compared with untransformed NIH 3T3 cells, we found a 2.26-fold increase in Rac-GTP levels in Vav2-transformed cells (Fig. 8). Thus, consistent with our *in vitro* GEF analyses, Vav2 causes constitutive up-regulation of Rac activity.

## DISCUSSION

Although the precise sequence requirements that dictate the GTPase specificity of DH domains remains to be delineated, our sequence alignment analyses of DH domain sequences showed a general relationship between sequence similarity and substrate utilization (2). Therefore, it was unexpected that Vav and Vav2, which share strong sequence identity in their DH domains, would possess GEF activity for distinct GTPase targets. Furthermore, it was found that activated Vav2 caused changes in cell morphology and actin cytoskeletal organization and a transformed phenotype that were distinct from those caused by activated Vav (18, 25). In contrast to these observations, we found that Vav and Vav2 share overlapping activities and that both can act as GEFs for RhoA, Rac1, and Cdc42.

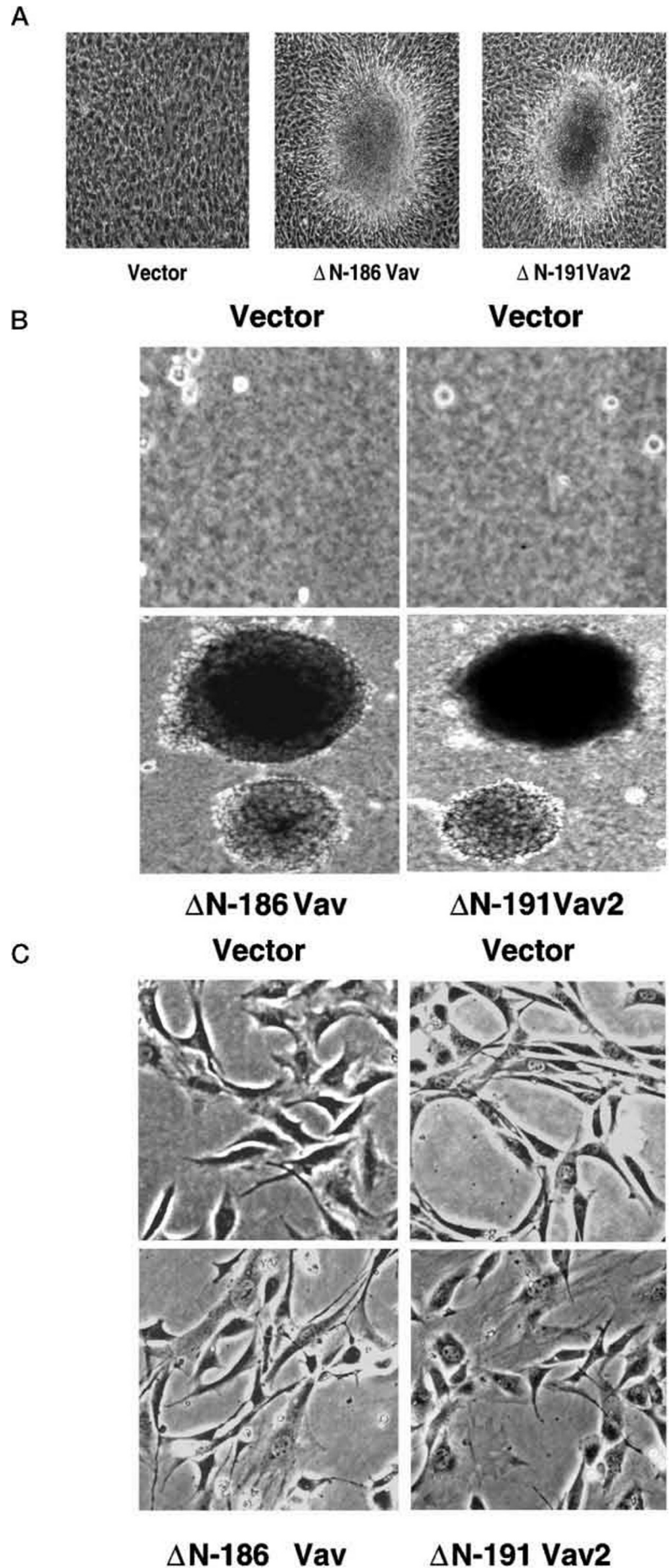


**FIG. 5. Dominant negative RhoA, Rac1, and Cdc42 block Vav2 focus-forming activity.** A, NIH 3T3 cells were transfected both with the pAX142 and the pZIP-NeoSV(x)1 mammalian expression vectors and with the pAX- $\Delta$ N-191 Vav2 (2  $\mu$ g) together with pZIP-NeoSV(x)1 (2  $\mu$ g) or pZIP-NeoSV(x)1 constructs encoding the wild-type or dominant negative mutants of RhoA (2  $\mu$ g), Rac1 (2  $\mu$ g), or Cdc42 (2  $\mu$ g), and Rho GAP p190 (2  $\mu$ g). B, the C3 exoenzyme inhibits Vav2 transforming activity. NIH 3T3 cells were transfected with pCDNA3 (2  $\mu$ g) and pAX142 vectors and with  $\Delta$ N-191 Vav2 (2  $\mu$ g) together with pCMV-C3 (2  $\mu$ g). C, the WASP-GBD blocks Vav2 transforming activity. NIH 3T3 cells were transfected with the pyDF30 (2  $\mu$ g) and pAX142 vectors and  $\Delta$ N-191 Vav2 (2  $\mu$ g) with pyDF30 (2  $\mu$ g) or pyDF30 WASP-GBD (2  $\mu$ g). Data shown are representative of at least three independent assays.

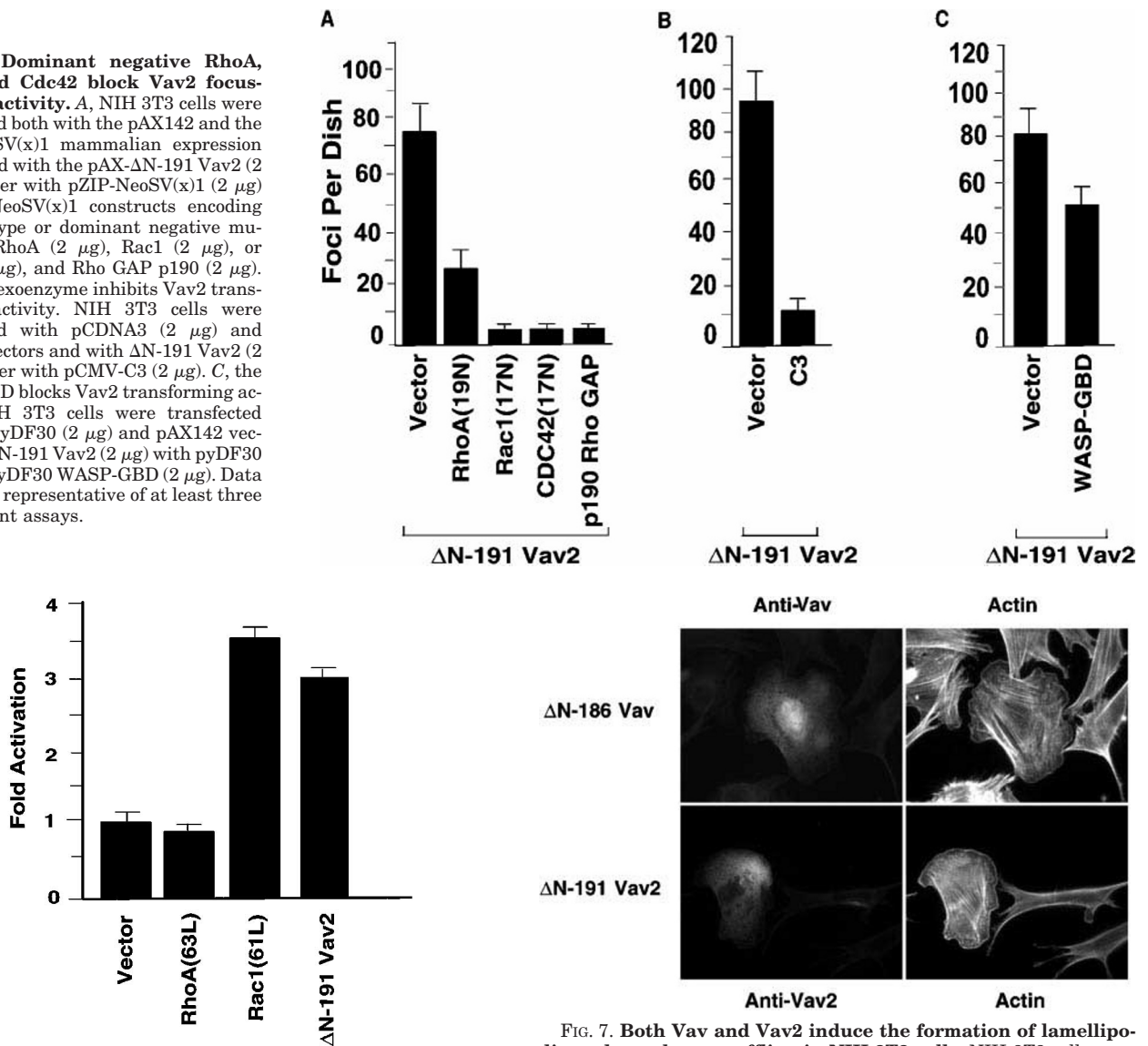


**FIG. 6. Vav2 activates c-Jun transcriptional activity.** NIH 3T3 cells were transiently transfected with the cognate empty pAX142 mammalian expression vector and pAX142 plasmids encoding the constitutively activated Rho(63L) (500 ng/dish), Rac1(61L) and  $\Delta$ N-191 Vav2, together with Gal4-Jun (250 ng/dish) and Gal4-Luc (2.5  $\mu$ g/dish). Data shown are representative of three independent assays.

First, we found that bacterially expressed fragments of the isolated DH or DH/PH/CRD domains of Vav2 exhibited GEF activity for RhoA, Rac1, and Cdc42 *in vitro*. Second, NH<sub>2</sub>-terminal truncated Vav2 caused the appearance of foci of transformed cells that were similar to those induced by NH<sub>2</sub>-terminal truncated and activated Vav. Vav- and Vav2-transformed NIH 3T3 cells were similar in morphologic appearance on plastic, and both displayed similar abilities to proliferate in soft agar. Third, we showed that Vav2 transforming activity was reduced by co-expression of various inhibitors of Rac1, RhoA, and Cdc42. Fourth, like Vav, Vav2 also activated c-Jun, a downstream target of the JNK mitogen-activated protein kinase. Rac1 and Cdc42, but not RhoA, are activators of JNK in NIH 3T3 cells. Fifth, like Vav, we also found that Vav2 could induce the formation of lamellipodia and membrane ruffles. Finally, we determined that Rac-GTP levels were constitutively up-regulated in Vav2-transformed cells. Thus, taken together, our data strongly suggest that Vav and Vav2 are activators of multiple, shared Rho family proteins.

Because Vav and Vav2 showed the most related sequence

**FIG. 7. Both Vav and Vav2 induce the formation of lamellipodia and membrane ruffling in NIH 3T3 cells.** NIH 3T3 cells were transfected with  $\Delta$ N-186 Vav or  $\Delta$ N-191 Vav2 and were analyzed by indirect immunofluorescence for changes in the actin cytoskeleton. An anti-Vav antibody (Santa Cruz Biotech) and an anti-Vav2 antibody were used to detect Vav or Vav2 expression. Lamellipodia induction and membrane ruffling were visualized using Texas Red-labeled phalloidin antibodies. Data shown are representative of three independent experiments.

relationship with each other in their DH domain sequences (2), we had anticipated that Vav and Vav2 would share similar, if not identical, GTPase targets for their GEF functions. During the course of our studies, Bustelo and colleagues (18) showed that Vav2 was an activator of RhoA, RhoB, and RhoG but not Rac1 or Cdc42 *in vitro*. In contrast, we found that Vav2 exhibited strong GEF activity for Rac1 and Cdc42, as well as for RhoA. Possible explanations for the different results between our group and Bustelo and colleagues may be the distinct types of Vav2 constructs utilized in the assays as well as the fact that we used human rather than mouse Vav2. For their *in vitro* GEF exchange assays, Bustelo and colleagues used insect cell-expressed, poly-histidine-tagged versions of either full-length or NH<sub>2</sub>-terminal truncated and activated Vav2. In contrast, we employed bacterially expressed versions of the isolated DH or DH/PH/CRD domains of Vav2. Thus, it is possible that COOH-terminal sequences, such as the SH3 and SH2 domains, may influence the GTPase substrate specificity of the DH domain.

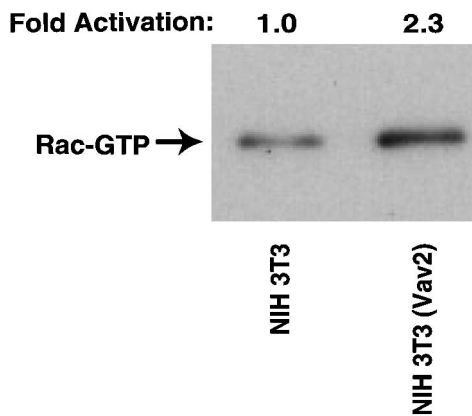


FIG. 8. Elevation of Rac-GTP levels in Vav2-transformed NIH 3T3 cells. The amount of activated Rac-GTP was determined in cell lysates of untransformed (empty vector-transfected) or Vav2-transformed NIH 3T3 cells by using bacterially expressed GST-PAK (residues 67–150) (47–49). The amount of Rac associated with GST-PAK was visualized by separation by 15% SDS-polyacrylamide gel electrophoresis and Western blot analysis with anti-Rac antibody (Signal Transduction Lab). Quantitation was done by densitometry scanning of the autoradiogram and the level of Rac-GTP for untransformed NIH 3T3 cells was normalized to one. Western blot analysis of the total cell lysate was also done to verify equivalent levels of endogenous Rac expressing in both cell populations (not shown). Data shown are representative of two independent assays.

However, Bustelo and colleagues, as well as our unpublished observations, showed that the SH domains were dispensable for Vav function *in vivo*. This would argue that the COOH-terminal SH2/SH3 domains do not play a significant role in dictating the substrate specificity of Vav and Vav2. Finally, changes in Rho GTPase substrate specificity may arise as a result of the different methods of protein expression (*E. coli* versus Sf9 cells) utilized that may result in distinct protein modifications.

In addition to differences in GTPase substrates, Bustelo and colleagues also found that Vav and Vav2 caused distinct transformed phenotypes, as well distinct changes in cellular morphology and actin cytoskeletal organization, when expressed in NIH 3T3 cells. However, in our transformation, signaling, and actin organization analyses, we found that NH<sub>2</sub>-terminal truncated versions of Vav and Vav2 caused essentially indistinguishable consequences. Furthermore, we found that like Vav,<sup>3</sup> Vav2 transforming activity was also dependent on the function of Rac1, RhoA, and Cdc42. Our signaling and actin cytoskeletal analyses also supported the possibility that Vav2 was an activator of Rac1 and/or Cdc42 *in vivo*. Like activated Rac1, Vav2 induced membrane ruffling and activation of JNK. Our cell-based analyses employed an activated version of Vav2 that retained all COOH-terminal sequences and was essentially identical to the one used in the previous study. Thus, we believe that our *in vitro* exchange results using the isolated DH or DH/PH/CRD domains of Vav2 do accurately reflect the GTPase specificity of authentic Vav2 *in vivo*. Therefore, we conclude that Vav and Vav2 are activators of overlapping and multiple small GTPases. At present, we do not have a clear explanation for why our conclusions contrast those described previously, except that our expression constructs, NIH 3T3 cell line (UNC strain), and assay conditions were not identical to those employed in their studies. In particular, we have found that different strains of NIH 3T3 cells respond differently to the same transforming protein (28).

Vav is activated in response to a very diverse spectrum of extracellular stimuli in a variety of hematopoietic cell types

(50). These stimuli include growth factors, cytokines, interleukins, and matrix components. At least some of these stimuli are believed to activate Vav by phosphorylation of an NH<sub>2</sub>-terminal tyrosine residue (Tyr<sup>174</sup>) (15), and this residue is also present in Vav2. Thus, it is likely that Vav2 will be activated by an equally diverse spectrum of extracellular stimuli in nonhematopoietic cells. Once activated, Vav and Vav2 are likely to mediate the same repertoire of downstream signaling events via activation of multiple small GTPases.

Like Vav, NH<sub>2</sub>-terminal truncation of the calponin homology and acidic domains results in conversion of Vav2 to a potent transforming protein. These two regions show strong sequence identity in Vav and Vav2 and are likely to contribute similarly to protein function. Although the exact mechanism by which the NH<sub>2</sub>-terminal sequences of Vav serve to negatively regulate function remains to be delineated, our recent analyses suggest that the NH<sub>2</sub> terminus may facilitate an intramolecular interaction with COOH-terminal sequences and modulate Vav membrane association (27). Whether the NH<sub>2</sub>-terminal sequences of Vav2 also serves an analogous function will be interesting to determine.

Vav and Vav2 share a similar array of COOH-terminal protein-protein or protein-lipid interaction domains. Following the PH domain is a cysteine-rich domain and tandem SH3 domains that flank a single SH2 domain. We recently found that deletion of the SH3/SH2/SH3 domains of activated Vav did not alter its transforming potential.<sup>3</sup> Thus, although a significant number of binding components have been identified that associate with these domains, these interactions are dispensable for Vav and Vav2 transformation. Vav and Vav2 do diverge in their COOH termini. Our sequence analyses identified a serine-rich region located within the Vav2 COOH terminus, after the SH2 domain (Fig. 1). This region (residues 769–811) is not present in Vav and comprises over 30% serine residues. This region also contains a consensus tyrosine phosphorylation site. Thus, further studies need to be performed to determine whether this region endows Vav2 with functional differences from those ascribed to Vav.

In summary, we have determined that like Vav, Vav2 is an activator of Rac1, RhoA, and Cdc42. Whether these two highly related Dbl family proteins serve the same functions in different cell types will require further elucidation of the extracellular signals that cause Vav2 activation. Additionally, although it is clear that Vav and Vav2 are activators of common small GTPases, whether they are distinct in their abilities to activate other Rho family proteins will be important to establish.

**Acknowledgments**—We thank Daniel Broek, Jeffrey Settleman, and Robert Weinberg for providing cDNA constructs sequence, Jennifer Parrish, and Misha Rand for preparation of figures and manuscript, and Carol Martin, Que Lambert, and Kelley Rogers-Graham for technical assistance.

#### REFERENCES

1. Cerione, R. A., and Zheng, Y. (1996) *Curr. Opin. Cell Biol.* **8**, 216–222
2. Whitehead, I. P., Campbell, S., Rossman, K. L., and Der, C. J. (1997) *Biochim. Biophys. Acta* **1332**, F1–F23
3. Narumiyama, S., Ishizaki, T., and Watanabe, N. (1997) *FEBS Lett.* **410**, 68–72
4. Van Aelst, L., and D'Souza-Schorey, C. (1997) *Genes Dev.* **11**, 2295–2322
5. Zohn, I. M., Campbell, S. L., Khosravi-Far, R., Rossman, K. L., and Der, C. J. (1998) *Oncogene* **17**, 1415–1438
6. Minden, A., Lin, A., Claret, F.-X., Abo, A., and Karin, M. (1995) *Cell* **81**, 1147–1157
7. Coso, O. A., Chiariello, M., Yu, J.-C., Teramoto, H., Crespo, P., Xu, N., Miki, T., and Gutkind, J. S. (1995) *Cell* **81**, 1137–1146
8. Perona, R., Montaner, S., Saniger, L., Sánchez-Pérez, I., Bravo, R., and Lacal, J. C. (1997) *Genes Dev.* **11**, 463–475
9. Hill, C. S., Wynne, J., and Treisman, R. (1995) *Cell* **81**, 1159–1170
10. Olson, M. F., Ashworth, A., and Hall, A. (1995) *Science* **269**, 1270–1272
11. Westwick, J. K., Lee, R. J., Lambert, Q. T., Symons, M., Pestell, R. G., Der, C. J., and Whitehead, I. P. (1998) *J. Biol. Chem.* **273**, 16739–16747
12. Whitehead, I. P., Khosravi-Far, R., Kirk, H., Trigo-Gonzalez, G., Der, C. J., and Kay, R. (1996) *J. Biol. Chem.* **271**, 18643–18650
13. Zheng, Y., Fischer, D. J., Santos, M. F., Tigy, G., Pasteris, N. G., Gorski, J. L.,

<sup>3</sup> K. Abe and C. J. Der, submitted for publication.



- and Xu, Y. (1996) *J. Biol. Chem.* **271**, 33169–33172
14. Michiels, F., Habets, G. G., Stam, J. C., van der Kammen, R. A., and Collard, J. G. (1995) *Nature* **375**, 338–340
  15. Han, J., Das, B., Wei, W., Van Aelst, L., Mosteller, R. D., Khosravi-Far, R., Westwick, J. K., Der, C. J., and Broek, D. (1997) *Mol. Cell. Biol.* **17**, 1346–1353
  16. Crespo, P., Schuebel, K. E., Ostrom, A. A., Gutkind, J. S., and Bustelo, X. R. (1997) *Nature* **385**, 169–172
  17. Olson, M. F., Pasteris, N. G., Gorski, J. L., and Hall, A. (1996) *Curr. Biol.* **6**, 1628–1633
  18. Schuebel, K. E., Movilla, N., Rosa, J. L., and Bustelo, X. R. (1998) *EMBO J.* **17**, 6608–6621
  19. Whitehead, I. P., Kirk, H., Tognon, C., Trigo-Gonzalez, G., and Kay, R. (1995) *J. Biol. Chem.* **270**, 18388–18395
  20. Whitehead, I. P., Lambert, Q. T., Glaven, J. A., Abe, K., Rossman, K. L., Mahon, G. M., Trzaskos, J. M., Kay, R., Campbell, S. L., and Der, C. J. (1999) *Mol. Cell. Biol.* **18**, 4689–4697
  21. Han, J., Luby-Phelps, K., Das, B., Shu, X., Xia, Y., Mosteller, R. D., Krishna, U. M., Falck, J. R., White, M. A., and Broek, D. (1998) *Science* **279**, 558–560
  22. Nimmual, A. S., Yatsula, B. A., and Bar-Sagi, D. (1998) *Science* **279**, 560–563
  23. Liu, X., Wang, H., Eberstadt, M., Schnuchel, A., Olejniczak, E. T., Meadows, R. P., Schkeryantz, J. M., Janowick, D. A., Harlan, J. E., Harris, E. A., Staunton, D. E., and Fesik, S. W. (1998) *Cell* **95**, 269–277
  24. Henske, E. P., Short, M. P., Jozwiak, S., Bovey, C. M., Ramlakhan, S., Haines, J. L., and Kwiatkowski, D. J. (1995) *Ann. Hum. Genet.* **59**, 25–37
  25. Schuebel, K. E., Bustelo, X. R., Nielsen, D. A., Song, B.-J., Barbacid, M., Goldman, D., and Lee, I. J. (1996) *Oncogene* **13**, 363–371
  26. Katzav, S., Cleveland, J. L., Heslop, H. E., and Pulido, D. (1991) *Mol. Cell. Biol.* **11**, 1912–1920
  27. Abe, K., Whitehead, I. P., O'Bryan, J. P., and Der, C. J. (1999) *J. Biol. Chem.* **274**, 30410–30418
  28. Khosravi-Far, R., White, M. A., Westwick, J. K., Solski, P. A., Chrzanoska-Wodnicka, M., Van Aelst, L., Wigler, M. H., and Der, C. J. (1996) *Mol. Cell. Biol.* **16**, 3923–3933
  29. Settleman, J., Albright, C. F., Foster, L. C., and Weinberg, R. A. (1992) *Nature* **359**, 153–154
  30. Symons, M., Derry, J. M. J., Karlak, B., Jiang, S., Lemahieu, V., McCormick, F., Francke, U., and Abo, A. (1996) *Cell* **84**, 723–734
  31. Qiu, R.-G., Abo, A., McCormick, F., and Symons, M. (1997) *Mol. Cell. Biol.* **17**, 3449–3458
  32. Clark, G. J., Cox, A. D., Graham, S. M., and Der, C. J. (1995) *Methods Enzymol.* **255**, 395–412
  33. Hauser, C. A., Der, C. J., and Cox, A. D. (1994) *Methods Enzymol.* **238**, 271–276
  34. Hauser, C. A., Westwick, J. K., and Quilliam, L. A. (1995) *Methods Enzymol.* **255**, 412–426
  35. Su, B., Jacinto, E., Hibi, M., Kallunki, T., Karin, M., and Ben-Neriah, Y. (1994) *Cell* **77**, 727–736
  36. Self, A. J., and Hall, A. (1995) *Methods Enzymol.* **256**, 3–10
  37. Campbell-Burk, S. L., and Carpenter, J. W. (1995) *Methods Enzymol.* **255**, 3–13
  38. Hart, M. J., Eva, A., Evans, T., Aaronson, S. A., and Cerione, R. A. (1991) *Nature* **354**, 311–314
  39. Leonard, D. A., Evans, T., Hart, M., Cerione, R. A., and Manor, D. (1994) *Biochemistry* **33**, 12323–12328
  40. Liu, B. P., Chrzanoska-Wodnicka, M., and Burridge, K. (1998) *Cell Adhes. Commun.* **5**, 249–255
  41. Ridley, A. J., Paterson, H. F., Johnston, C. L., Diekmann, D., and Hall, A. (1992) *Cell* **70**, 401–410
  42. Ridley, A. J., and Hall, A. (1992) *Cell* **70**, 389–399
  43. Nobes, C. D., and Hall, A. (1995) *Cell* **81**, 53–62
  44. Whitehead, I. P., Abe, K., Gorski, J. L., and Der, C. J. (1998) *Mol. Cell. Biol.* **18**, 4689–4697
  45. Settleman, J., Narasimhan, V., Foster, L. C., and Weinberg, R. A. (1992) *Cell* **69**, 539–549
  46. Crespo, P., Bustelo, X. R., Aaronson, D. S., Coso, O. A., Lopez-Barahona, M., Barbacid, M., and Gutkind, J. S. (1996) *Oncogene* **13**, 455–460
  47. Sander, E. E., van Delft, S., ten Klooster, J. P., Reid, T., van der Kammen, R. A., Michiels, F., and Collard, J. G. (1998) *J. Cell Biol.* **143**, 1385–1398
  48. Benard, V., Bohl, B. P., and Bokoch, G. M. (1999) *J. Biol. Chem.* **274**, 13198–13204
  49. Bagroli, S., Taylor, S. J., Jordon, K. A., Van Aelst, L., and Cerione, R. A. (1998) *J. Biol. Chem.* **273**, 23633–23636
  50. Bustelo, X. R. (1996) *Crit. Rev. Oncog.* **7**, 65–88